

## A CERTAIN MIXED BOUNDARY VALUE PROBLEM FOR A BIMATERIAL INTERFACE

ROBERTO BALLARINI

Department of Civil Engineering, Case Western Reserve University, Cleveland,  
OH 44106-7201, U.S.A.

(Received 7 June 1994)

**Abstract**—This paper presents the solution of a certain mixed problem for a bimaterial interface containing a cut. In the plane, elastostatic analysis displacements are prescribed on the lower edge of the cut and external stresses are applied on its upper edge. Using complex variable techniques, analytical expressions are derived for all physical quantities, including the compliance of the anchor, the stress field, and the stress singularities at its edges. Selected numerical values are presented for these quantities as functions of elastic mismatch. The developed solution can be used to model a vertically loaded rigid anchor, unbonded on one side, embedded along the interface between two elastic materials.

### 1. INTRODUCTION

The mechanical behavior of anchors embedded in brittle materials is an important consideration for many critical design situations. Most of the analytical models that have been developed to estimate the mechanical response of embedded anchors focused primarily on stress distributions and load deflection behavior (Sherman, 1940; Muki and Sternberg, 1970; Butterfield and Banerjee, 1971; Keer, 1975; Selvadurai, 1976; Bosakov, 1980; Luk and Keer, 1980; Pak and Gobert, 1990). Recent efforts to predict the pull-out capacity of anchor bolts have included the cracking that often emanates from the edge(s) of the anchor and grows towards a free surface (Ballarini *et al.*, 1986, 1987).

In the aforementioned analyses the anchor was surrounded by a homogeneous isotropic linear elastic matrix. This paper presents the solution to the plane elastostatics problem shown in Fig. 1(a). A very thin rigid plate is embedded along the interface between two dissimilar semi-infinite planes and is loaded by a vertical force. One side of the plate is debonded (from the material in the upper half-plane), while the other side is perfectly bonded to the material in the lower half-plane. Because the plate is assumed very thin, its effects on the surrounding medium can be approximated with those produced by a bimaterial interface containing a cut, with displacements prescribed on the lower edge and stresses prescribed on the upper edge. Of particular interest is the effect of elastic mismatch on the compliance of the anchor, the stress field, and the stress singularities at the edges of the anchor.

The corresponding plane problem for the homogeneous medium was first solved by Sherman (1940) using singular integral equations. An omission in his solution was pointed out by Muskhelishvili, who derived the solution by reducing the problem to two uncoupled Hilbert problems. The solution to the penny-shaped cut was presented by Keer (1975). An interesting feature of these solutions is that there are two stress singularities at the edge of the plate, one equal to  $-1/4 + i \log \kappa/4\pi$ , the other to  $-3/4 + i \log \kappa/4\pi$ , where  $\kappa = 3 - 4\nu$  for plane strain and  $\kappa = (3 - \nu)/(1 - \nu)$  for plane stress.

The solution presented in this paper relies on a set of potentials that reduce the boundary conditions to a Hilbert problem, whose solution is obtained in closed form. These potentials are presented in the following section.

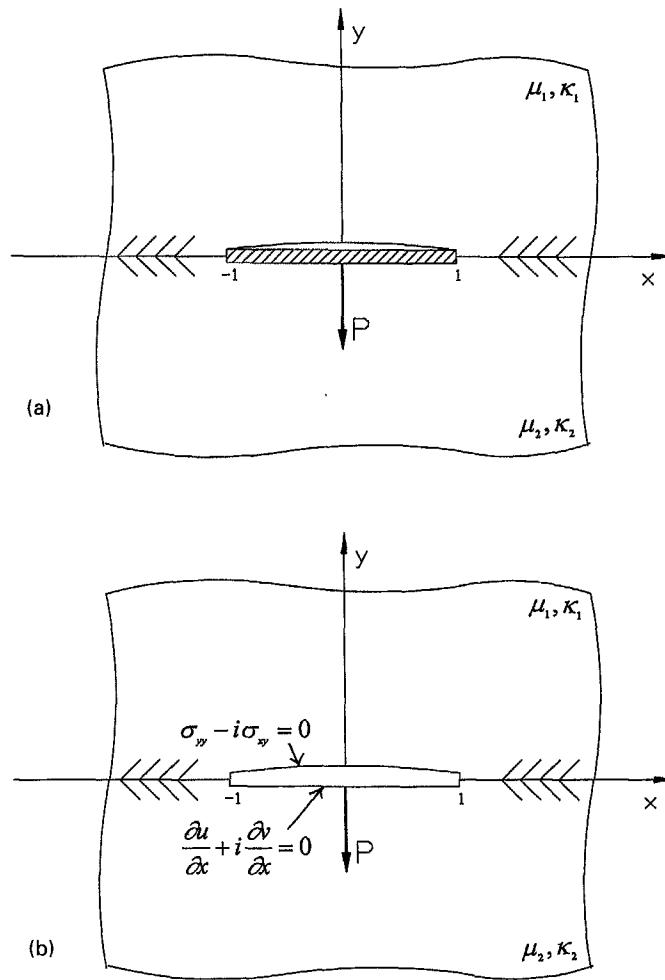


Fig. 1. (a) Thin anchor along a bimaterial interface; (b) bimaterial interface containing a cut with stresses (displacements) prescribed on upper (lower) edge.

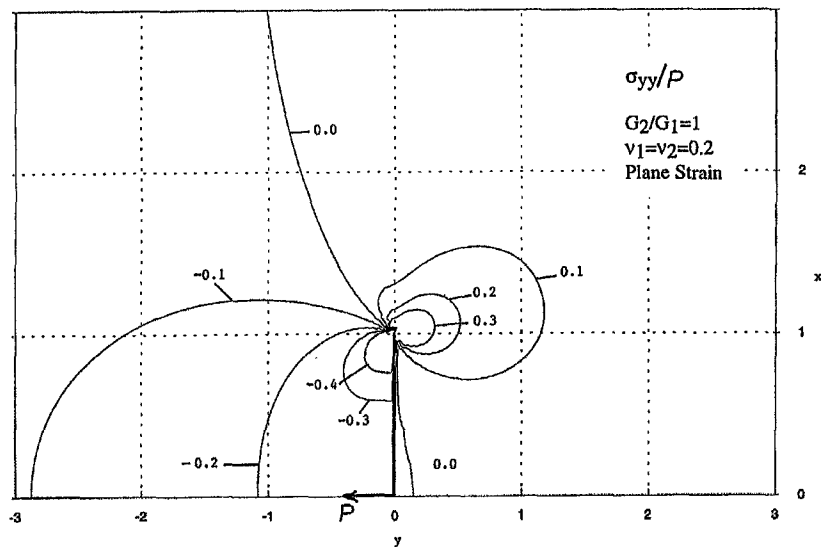


Fig. 2.  $\sigma_{yy}/P$  for plane strain ( $\mu_2/\mu_1 = 1, \nu_1 = \nu_2 = 0.2$ ).

2. ANALYTIC CONTINUATION METHOD FOR A BIMATERIAL INTERFACE

This section presents an analytic continuation procedure that can be used to formulate problems associated with a bimaterial interface containing a cut. The advantage of the method is that it eliminates the need to develop the Green's functions for a dislocation and a point force at the interface, and the associated singular integral equations. The method essentially generalizes the procedure outlined in Muskhelishvili's treatment of Sherman's problem.

Consider the class of plane elastostatics problems associated with the upper half-plane  $S^+$  with moduli  $\mu_1$  and  $\nu_1$  and the lower half-plane  $S^-$  with moduli  $\mu_2$  and  $\nu_2$ , where  $\mu_i$  and  $\nu_i, i = 1, 2$ , denote the shear modulus and Poisson ratio, respectively.

The stresses and displacements may be expressed in terms of the Muskhelishvili potentials (Muskhelishvili, 1953) as follows:

$$(\sigma_{yy} - i\sigma_{xy})_i = \Phi_i(z) + \overline{\Phi_i(z)} + z\overline{\Phi_i'(z)} + \overline{\Psi_i(z)} \tag{1}$$

$$(\sigma_{yy} + \sigma_{xx})_i = 2[\Phi_i(z) + \overline{\Phi_i(z)}] \tag{2}$$

$$2\mu_i \left( \frac{\partial u}{\partial x} + i \frac{\partial v}{\partial x} \right)_i = \kappa_i \Phi_i(z) - [\overline{\Phi_i(z)} + z\overline{\Phi_i'(z)} + \overline{\Psi_i(z)}]. \tag{3}$$

The subscript  $i$  ( $i = 1, 2$ ) denotes "in region  $S_i$ ";  $\Phi_1$  and  $\Psi_1$  correspond to the potentials for the upper half-plane and  $\Phi_2$  and  $\Psi_2$  correspond to the potentials for the lower half-plane. Moreover,  $z$  is the complex variable  $x + iy$ , the prime denotes differentiation with respect to  $z$ , and an overbar denotes complex conjugation.

As shown by Mukai *et al.* (1990), for such interface problems it is more convenient to introduce additional "jump" potentials as follows. Making use of the fact that if  $f(z)$  is analytic for  $z$  in region  $R$ , then  $\bar{f}(z) \equiv \overline{f(\bar{z})}$  is analytic for  $\bar{z}$  in region  $R$ , the following analytic potentials are constructed:

$$\Omega_s(z) = \begin{cases} \Phi_1(z) - [\overline{\Phi_2(z)} + z\overline{\Phi_2'(z)} + \overline{\Psi_2(z)}] & z \in S_1 \\ \Phi_2(z) - [\overline{\Phi_1(z)} + z\overline{\Phi_1'(z)} + \overline{\Psi_1(z)}] & z \in S_2 \end{cases} \tag{4}$$

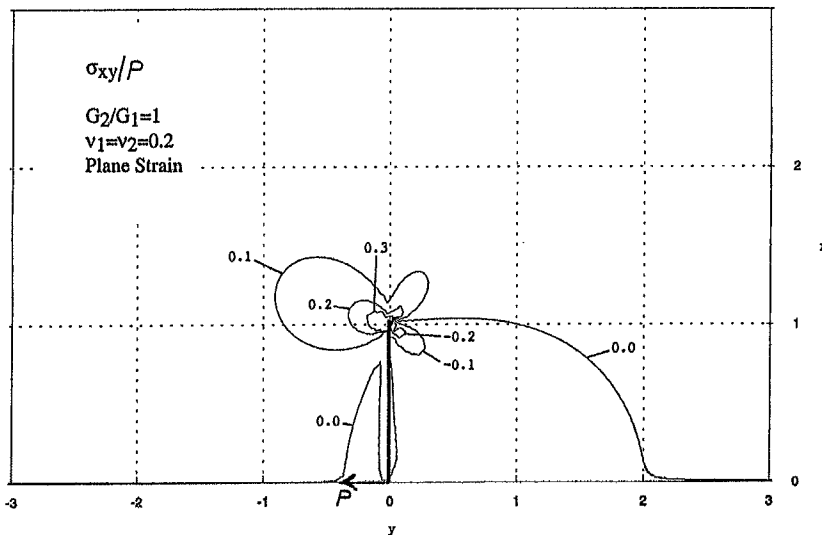


Fig. 3.  $\sigma_{xy}/P$  for plane strain ( $\mu_2/\mu_1 = 1, \nu_1 = \nu_2 = 0.2$ ).

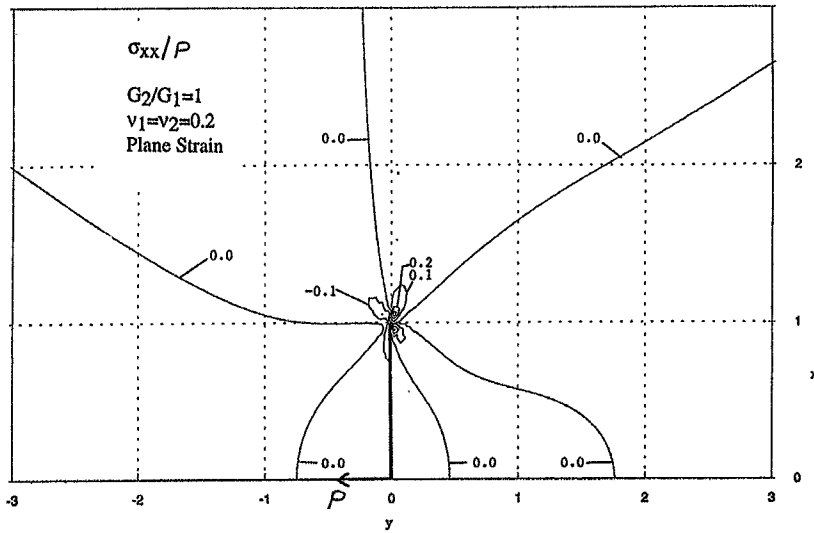


Fig. 4.  $\sigma_{xx}/P$  for plane strain ( $\mu_2/\mu_1 = 1, \nu_1 = \nu_2 = 0.2$ ).

$$\Omega_d(z) = \begin{cases} \frac{\kappa_1}{2\mu_1} \Phi_1(z) + \frac{1}{2\mu_2} [\bar{\Phi}_2(z) + z\bar{\Phi}'_2(z) + \bar{\Psi}_2(z)] & z \in S_1 \\ \frac{\kappa_2}{2\mu_2} \Phi_2(z) + \frac{1}{2\mu_1} [\bar{\Phi}_1(z) + z\bar{\Phi}'_1(z) + \bar{\Psi}_1(z)] & z \in S_2. \end{cases} \quad (5)$$

In terms of these potentials the discontinuities in stresses and displacements across the interface are given by

$$(\sigma_{yy} - i\sigma_{xy})^+ - (\sigma_{yy} - i\sigma_{xy})^- = \Omega_s^+(x) - \Omega_s^-(x) \quad (6)$$

$$\left(\frac{\partial u}{\partial x} + i\frac{\partial v}{\partial x}\right)^+ - \left(\frac{\partial u}{\partial x} + i\frac{\partial v}{\partial x}\right)^- = \Omega_d^+(x) - \Omega_d^-(x). \quad (7)$$

The superscript  $+$  ( $-$ ) represents the limit as the interface is approached from region  $S_1$  ( $S_2$ ). It is obvious from these last two equations that the discontinuities in the potentials represent, respectively, force and dislocation distributions along the interface. Equations

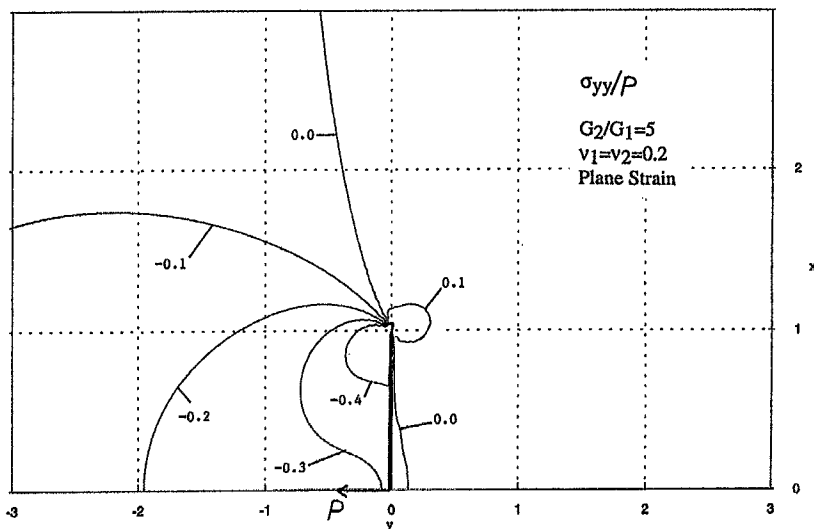


Fig. 5.  $\sigma_{yy}/P$  for plane strain ( $\mu_2/\mu_1 = 5, \nu_1 = \nu_2 = 0.2$ ).

(4) and (5) can be readily inverted to recover the potentials that appear in eqns (1)–(3). The resulting representations become

$$\Phi_1(z) = \frac{2\mu_1\mu_2}{\mu_1 + \mu_2\kappa_1} \left[ \frac{1}{2\mu_2} \Omega_s(z) + \Omega_d(z) \right] \tag{8}$$

$$\Psi_1(z) = \frac{2\mu_1\mu_2}{\mu_2 + \mu_1\kappa_2} \left[ \frac{-\kappa_2}{2\mu_2} \bar{\Omega}_s(z) + \bar{\Omega}_d(z) \right] - \Phi_1(z) - z\Phi_1'(z) \tag{9}$$

$$\Phi_2(z) = \frac{2\mu_1\mu_2}{\mu_2 + \mu_1\kappa_2} \left[ \frac{1}{2\mu_1} \Omega_s(z) + \Omega_d(z) \right] \tag{10}$$

$$\Psi_2(z) = \frac{2\mu_1\mu_2}{\mu_1 + \mu_2\kappa_1} \left[ \frac{-\kappa_1}{2\mu_1} \bar{\Omega}_s(z) + \bar{\Omega}_d(z) \right] - \Phi_2(z) - z\Phi_2'(z). \tag{11}$$

### 3. BOUNDARY CONDITIONS AND REDUCTION TO UNCOUPLED HILBERT PROBLEMS

Equations (6) and (7) clearly demonstrate the usefulness of the jump potentials for solving problems involving an interface containing a cut. For example, the interface *crack* can be treated by setting the discontinuity in stress equal to zero and solving for the crack opening displacements. The solution of the *rigid line inclusion* problem, which was obtained by Ballarini (1990), can be derived by setting the discontinuity in displacement equal to zero and solving for the stress distribution along the rigid inclusion.

The boundary conditions for the configuration shown in Fig. 1(b) are written as

$$(\sigma_{yy} - i\sigma_{xy})^+ = 0 = \frac{\mu_1}{\mu_1 + \mu_2\kappa_1} \Omega_s^+ + \frac{2\mu_1\mu_2}{\mu_1 + \mu_2\kappa_1} \Omega_d^+(x) - \frac{\mu_1\kappa_2}{\mu_2 + \mu_1\kappa_2} \Omega_s^-(x) + \frac{2\mu_1\mu_2}{\mu_2 + \mu_1\kappa_2} \Omega_d^-(x), \quad |x| < 1, y = 0 \tag{12}$$

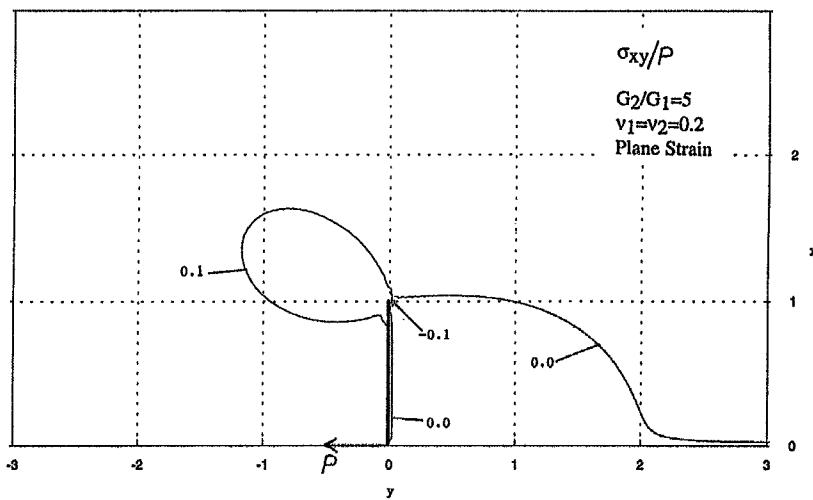


Fig. 6.  $\sigma_{xy}/P$  for plane strain ( $\mu_2/\mu_1 = 5, \nu_1 = \nu_2 = 0.2$ ).

$$\left(\frac{\partial u}{\partial x} + i\frac{\partial v}{\partial x}\right)^- = 0 = \frac{\mu_2\kappa_2}{\mu_2 + \mu_1\kappa_2}\Omega_s^-(x) + \frac{2\kappa_2\mu_1\mu_2}{\mu_2 + \mu_1\kappa_2}\Omega_d^-(x) + \frac{\mu_2\kappa_1}{\mu_1 + \mu_2\kappa_1}\Omega_s^+(x) - \frac{2\mu_1\mu_2}{\mu_1 + \mu_2\kappa_1}\Omega_d^+(x), \quad |x| < 1, y = 0 \quad (13)$$

$$(\sigma_{yy} - i\sigma_{xy})^+ - (\sigma_{yy} - i\sigma_{xy})^- = \Omega_s^+(x) - \Omega_s^-(x) = 0, \quad |x| > 1, y = 0 \quad (14)$$

$$\left(\frac{\partial u}{\partial x} + i\frac{\partial v}{\partial x}\right)^+ - \left(\frac{\partial u}{\partial x} + i\frac{\partial v}{\partial x}\right)^- = \Omega_d^+(x) - \Omega_d^-(x) = 0, \quad |x| > 1, y = 0. \quad (15)$$

Equations (12) and (13) represent the zero traction and rigid anchor conditions along the cut, respectively, while eqns (14) and (15) represent the perfect bond along the remaining part of the interface. A unique solution is obtained by applying the following equilibrium and single valued displacement conditions:

$$\int_{-1}^1 [(\sigma_{yy} - i\sigma_{xy})^+ - (\sigma_{yy} - i\sigma_{xy})^-] dx = \int_{-1}^1 (\Omega_s^+(x) - \Omega_s^-(x)) dx = P \quad (16)$$

$$\int_{-1}^1 \left[ \left(\frac{\partial u}{\partial x} + i\frac{\partial v}{\partial x}\right)^+ - \left(\frac{\partial u}{\partial x} + i\frac{\partial v}{\partial x}\right)^- \right] dx = \int_{-1}^1 (\Omega_d^+(x) - \Omega_d^-(x)) dx = 0. \quad (17)$$

It should be noted that the problem could have been reduced to eqns (12)–(17) in a less direct way by starting out with the Green's functions for a concentrated force and a discrete dislocation at the interface, replacing these with distributions, and writing the boundary conditions in terms of singular integral equations. Equations (12) and (13) would subsequently be recovered by applying the Plemelj formulae to the singular integral equations.

Although it is not immediately apparent, eqns (12)–(15) define a Hilbert problem. That is, eqns (12) and (13) can be cast in the form

$$[A\Omega_s(x) + B\Omega_d(x)]^+ - \lambda[A\Omega_s(x) + B\Omega_d(x)]^- = 0 \quad (18)$$

using the process outlined by Clements (1971), which involves multiplying eqn (13) by  $N$ , adding the result to eqn (12), and applying eqn (18). The procedure leads to the eigenvalue problem

$$[\Omega_s^-(x) \quad \Omega_d^-(x)] \begin{bmatrix} \lambda - \kappa_2 m & \lambda \kappa_1 + \kappa_2 m \\ (\lambda + m)\mu_2 & -\mu_1(\lambda - \kappa_2 m) \end{bmatrix} \begin{Bmatrix} 1 \\ N \end{Bmatrix} = 0, \quad (19)$$

where  $m = (1 + \beta)/(1 - \beta)$ . This last equation in turn provides the characteristic equation

$$\lambda^2 + \lambda \left[ \kappa_2 \left( \frac{\alpha - \beta}{1 - \beta} \right) + \frac{\alpha + \beta}{1 - \beta} \right] + \left( \frac{1 + \beta}{1 - \beta} \right) \kappa_2 = 0, \quad (20)$$

where  $\alpha$  and  $\beta$  are the Dundurs constants defined as

$$\alpha = \frac{\mu_2(\kappa_1 + 1) - \mu_1(\kappa_2 + 1)}{\mu_2(\kappa_1 + 1) + \mu_1(\kappa_2 + 1)} \quad (21)$$

$$\beta = \frac{\mu_2(\kappa_1 - 1) - \mu_1(\kappa_2 - 1)}{\mu_2(\kappa_1 + 1) + \mu_1(\kappa_2 + 1)}. \quad (22)$$

The two roots of eqn (20),  $\lambda_1$  and  $\lambda_2$ , are associated with two values of  $N_i$  ( $i = 1, 2$ ), which are obtained in terms of the eigenvalues through eqn (19). These in turn can be used to find the corresponding values of  $A_i, B_i$ . Some trivial manipulations lead to

$$N_i = \frac{-\lambda_i(1-\beta) + \kappa_2(1+\beta)}{\lambda_i\kappa_i(1-\beta) + \kappa_2(1+\beta)} \tag{23}$$

$$A_i = 1 + \kappa_1 N_i, \quad B_i = 2(\mu_2 - \mu_1 N_i). \tag{24}$$

At this point all the constants that appear in eqn (18) have been determined. The solution of these equations is given by (Muskhelishvili, 1953)

$$A_i\Omega_s(z) + B_i\Omega_d(z) = k_i X_i(z), \quad i = 1, 2, \tag{25}$$

where

$$X_i(z) = (z+1)^{-\gamma_i}(z-1)^{\gamma_i-1}, \quad \gamma_i = \frac{\log(\lambda_i)}{2\pi i}. \tag{26}$$

Thus

$$\Omega_s(z) = \frac{k_1 B_2 X_1(z) - k_2 B_1 X_2(z)}{A_1 B_2 - A_2 B_1}, \quad \Omega_d(z) = \frac{-k_1 A_2 X_1(z) + k_2 A_1 X_2(z)}{A_1 B_2 - A_2 B_1}. \tag{27}$$

The identities

$$X_i^+(x) = \lambda_i X_i^-(x) = (1+x)^{-\lambda_i} (1-x)^{\lambda_i-1} e^{i\pi(\lambda_i-1)} \tag{28}$$

and

$$\int_{-1}^1 (1+x)^{-\gamma} (1-x)^{\gamma-1} dx = \frac{\pi}{\sin \pi\gamma} \tag{29}$$

allows eqns (16) and (17) to be written as

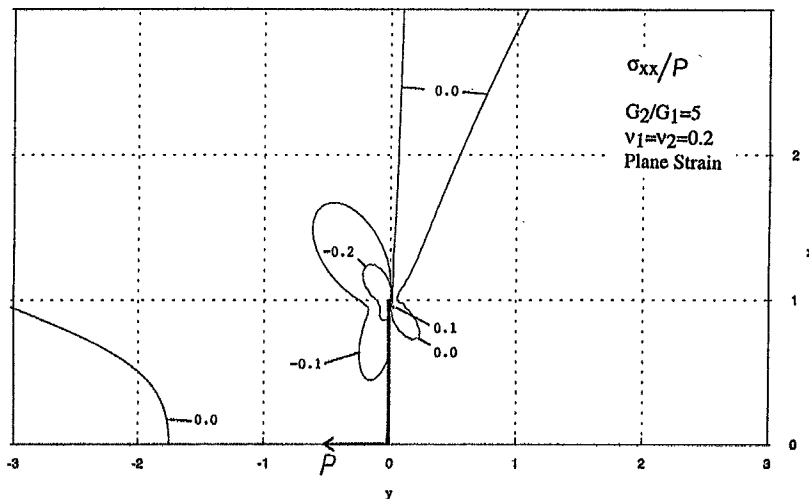


Fig. 7.  $\sigma_{xx}/P$  for plane strain ( $\mu_2/\mu_1 = 5, \nu_1 = \nu_2 = 0.2$ ).

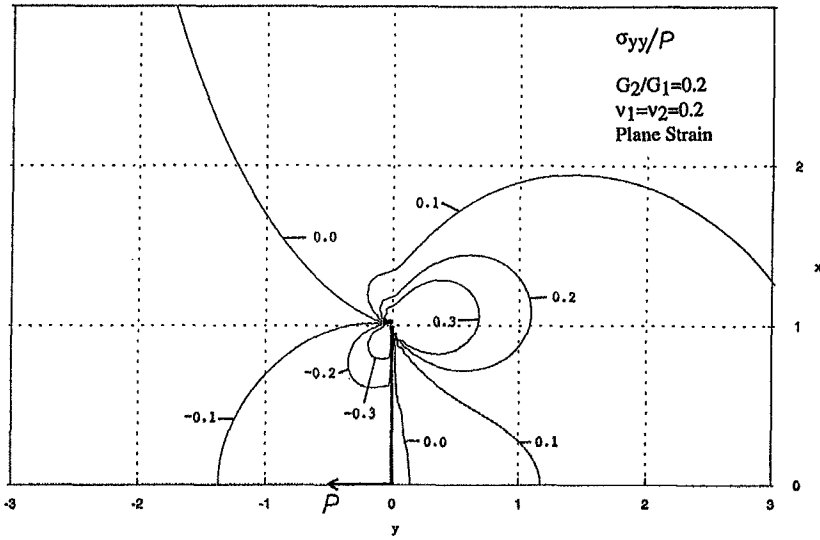


Fig. 8.  $\sigma_{yy}/P$  for plane strain ( $\mu_2/\mu_1 = 0.2, \nu_1 = \nu_2 = 0.2$ ).

$$\begin{bmatrix} \frac{B_2 e^{i\pi(\gamma_1-1)} (1-\lambda_1^{-1})}{\sin \pi\gamma_1} & -\frac{B_1 e^{i\pi(\gamma_2-1)} (1-\lambda_2^{-1})}{\sin \pi\gamma_2} \\ -\frac{A_2 e^{i\pi(\gamma_1-1)} (1-\lambda_1^{-1})}{\sin \pi\gamma_1} & \frac{A_1 e^{i\pi(\gamma_2-1)} (1-\lambda_2^{-1})}{\sin \pi\gamma_2} \end{bmatrix} \begin{Bmatrix} k_1 \\ k_2 \end{Bmatrix} = \begin{Bmatrix} \frac{P}{n} (A_1 B_2 - A_2 B_1) \\ 0 \end{Bmatrix}, \quad (30)$$

which provides constants  $k_i$ . All physical quantities can now be calculated with the closed form expressions for the potentials  $\Omega_s(z)$  and  $\Omega_d(z)$ . In particular, the crack opening displacement at the middle of the anchor is given by

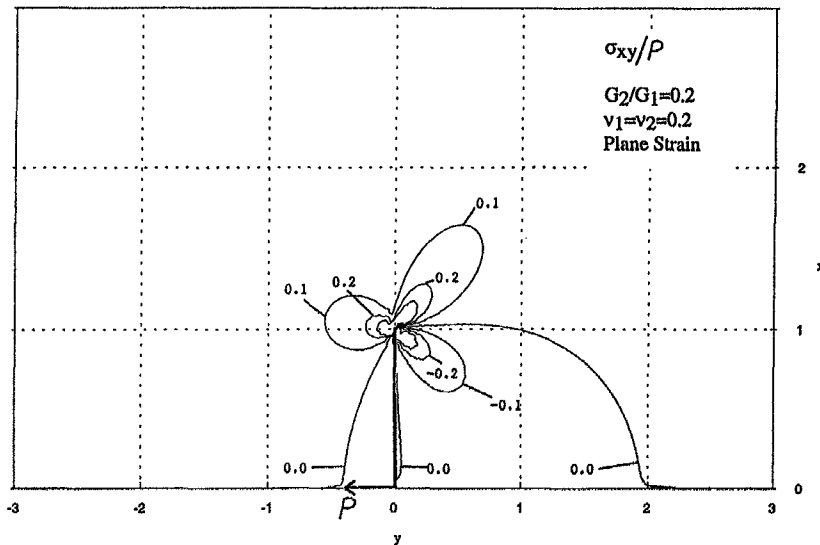


Fig. 9.  $\sigma_{xy}/P$  for plane strain ( $\mu_2/\mu_1 = 0.2, \nu_1 = \nu_2 = 0.2$ ).



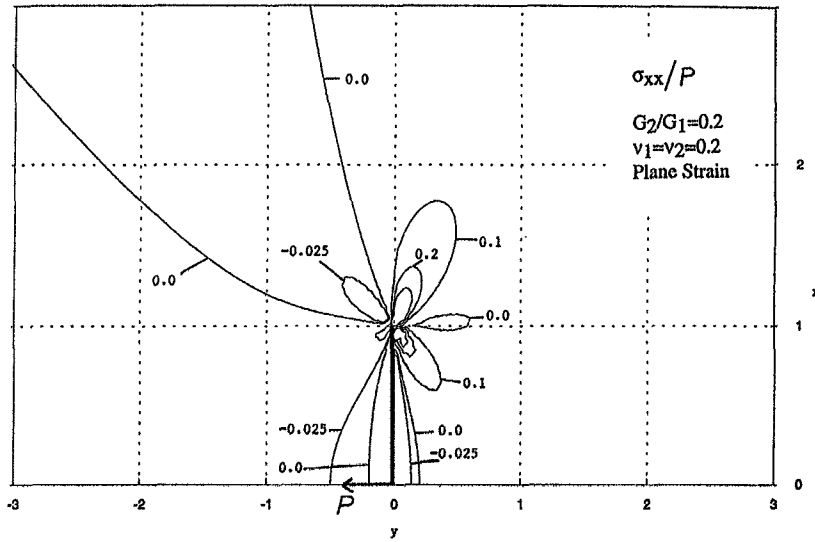


Fig. 10.  $\sigma_{xx}/P$  for plane strain ( $\mu_2/\mu_1 = 0.2, \nu_1 = \nu_2 = 0.2$ ).

$$\Delta = \int_0^1 (\Omega_d^+(x) - \Omega_d^-(x)) dx = \frac{1}{A_1 B_2 - A_2 B_1} \left\{ -A_2 k_1 e^{i\pi(\nu_1-1)} \left(1 - \frac{1}{\lambda_1}\right) \times \frac{{}_2F_1(1, \gamma_1; 1 + \gamma_1; -1)}{\gamma_1} + A_1 k_2 e^{i\pi(\nu_2-1)} \left(1 - \frac{1}{\lambda_2}\right) \frac{{}_2F_1(1, \gamma_2; 1 + \gamma_2; -1)}{\gamma_2} \right\}, \quad (31)$$

where  ${}_2F_1(1, \gamma; 1 + \gamma; -1)$  is the hypergeometric function that can be calculated from the identity

$${}_2F_1(1, \gamma; 1 + \gamma; -1) = \gamma \sum_{n=0}^{\infty} (-1)^n (\gamma + n)^{-1}. \quad (32)$$

#### 4. SELECTED RESULTS

For plane strain conditions with  $\nu_1 = \nu_2 = 0.2$ , eqns (31), (1), (2) and (6) were evaluated for selected values of  $\mu_2/\mu_1$ . The strengths of the singularities at the edges of the plate and

Table 1. Stress singularities and crack opening displacement

$\mu_2/\mu_1$	$\gamma_1$	$\gamma_2$	$\Delta\mu_1/P$
0.2	0.1398 - 0.0221i	0.8602 - 0.0221i	0.6437
0.3	0.1649 - 0.0302i	0.8351 - 0.0302i	0.4946
0.4	0.1841 - 0.0369i	0.8159 - 0.0369i	0.4073
0.5	0.1996 - 0.0427i	0.8004 - 0.0427i	0.3487
0.6	0.2126 - 0.0478i	0.7874 - 0.0478i	0.3062
0.7	0.2238 - 0.0522i	0.7762 - 0.0522i	0.2738
0.8	0.2336 - 0.0561i	0.7664 - 0.0561i	0.2480
0.9	0.2422 - 0.0596i	0.7578 - 0.0596i	0.2270
1	0.2500 - 0.0627i	0.7500 - 0.0627i	0.2095
2	0.3004 - 0.0827i	0.6996 - 0.0827i	0.1206
3	0.3282 - 0.0929i	0.6718 - 0.0929i	0.0856
4	0.3467 - 0.0992i	0.6533 - 0.0992i	0.0665
5	0.3602 - 0.1034i	0.6398 - 0.1034i	0.0545
6	0.3706 - 0.1064i	0.6294 - 0.1064i	0.0462
7	0.3790 - 0.1087i	0.6210 - 0.1087i	0.0401
8	0.3859 - 0.1106i	0.6141 - 0.1106i	0.0354
9	0.3917 - 0.1120i	0.6083 - 0.1120i	0.0317
10	0.3968 - 0.1132i	0.6032 - 0.1132i	0.0287

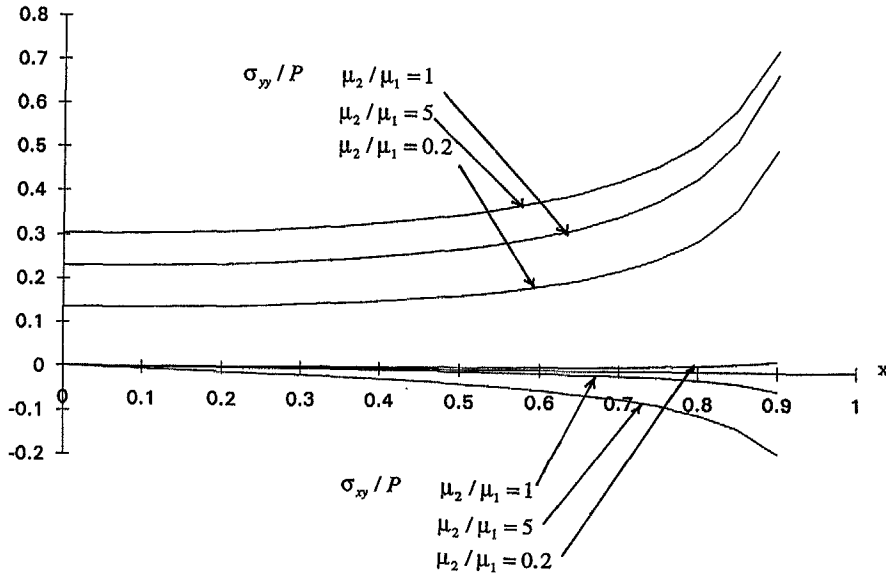


Fig. 11. Contact stress distribution along the anchor.

the normalized crack opening displacement at the middle of the anchor are presented in Table 1. It is observed that the boundary conditions assumed along the cut lead to two “oscillating singularities”, which predict interpenetration of material, as discussed by Comninou and Dundurs (1980). While it is beyond the scope of this paper, this contradiction can be avoided by requiring that certain inequalities be incorporated into the formulation, as was done for interface cracks in a series of papers by Comninou and Dundurs (Comninou, 1977a,b, 1978; Comninou and Dundurs, 1979a,b, 1980; Dundurs and Comninou, 1979). They introduced contact zones of length  $c$  at the tips of an interface crack of length  $2l$  and found that, for tensile loading,  $(l-c)/l$  is of the order of  $10^{-4}$ . Moreover, the global features of the stress field were found to be practically the same as those of the interface crack with no contact zones. These results suggest that, for the vertically loaded anchor analysed in this paper, the analytic solution can be used to study the global features of the stress field, but not the stress distribution in the immediate vicinity of the crack tips.

As expected the compliance of the anchor decreases as the stiffness of the lower half-plane increases.

Figures 2–10 are contour plots of the Cartesian stress components, normalized by multiplying their values by the half-length of the anchor (which is equal to 1), and dividing by the vertical load  $P$ . Figures 2, 5 and 8 show, as expected, that as the stiffness of the lower half-plane increases (decreases), the compression in the lower half-plane increases (decreases), while the tension in the upper half-plane decreases (increases). Similar trends for the magnitudes of the other stress components are observed by comparing Figs 3, 6 and 9 and Figs 4, 7 and 10.

The contact stress distribution (6) is shown in Fig. 11. An interesting feature of the solution is that the shear stress needed to satisfy the rigid line boundary conditions is relatively small. At first sight it seems that the area under each normal stress distribution is not equal to the applied load. It should be noted, however, that the strength of the singularity at the tips of the anchor increases with decreasing  $\mu_2/\mu_1$ , and that the normal stress curves in Fig. 11 cross somewhere within the interval  $0.9 < x < 1.0$ .

*Acknowledgement*—This work was supported by NASA-Lewis under Grant NAG3-856.

#### REFERENCES

- Ballarini, R. (1990). A rigid line inclusion at a bimaterial interface. *Engng Fract. Mech.* **37**, 1–5.  
 Ballarini, R., Shah, S. P. and Keer, L. M. (1986). Failure characteristics of short anchor bolts embedded in a brittle material. *Proc. R. S. London* **A404**, 35–54.

- Ballarini, R., Keer, L. M. and Shah, S. P. (1987). An analytical model for the pull-out of rigid anchors. *Int. J. Fract.* **33**, 75–94.
- Bosakov, S. V. (1980). *Prikl. Mekh.* **16**, 81–87.
- Butterfield, R. and Banerjee, P. K. (1971). A rigid disc embedded in an elastic half-space. *Geotech. Engng* **2**, 35–49.
- Clements, D. L. (1971). A crack between dissimilar anisotropic media. *Int. J. Engng Sci.* **9**, 257–265.
- Comninou, M. (1977a). Interface crack with friction in the contact zone. *ASME J. Appl. Mech.* **44**, 780–781.
- Comninou, M. (1977b). The interface crack. *ASME J. Appl. Mech.* **44**, 631–636.
- Comninou, M. (1978). The interface crack in a shear field. *ASME J. Appl. Mech.* **45**, 287–290.
- Comninou, M. and Dundurs, J. (1979a). On the frictional contact in crack analysis. *Engng Fract. Mech.* **12**, 117–123.
- Comninou, M. and Dundurs, J. (1979b). An example for frictional slip progressing into a contact zone of a crack. *Engng Fract. Mech.* **12**, 191–197.
- Comninou, M. and Dundurs, J. (1980). On the behavior of interface cracks. *Res. Mech.* **1**, 249–264.
- Dundurs, J. and Comninou, M. (1979). Some consequences of the inequality conditions in contact and crack problems. *J. Elasticity* **9**, 71–82.
- Keer, L. M. (1975). Mixed boundary value problems for a penny-shaped cut. *J. Elasticity* **5**, 89–98.
- Luk, V. K. and Keer, L. M. (1980). *Int. J. Numer. Meth. Geomech.* **4**, 215–232.
- Muki, R. and Sternberg, E. (1970). Elastostatic load-transfer to a half-space from a partially embedded axially loaded rod. *Int. J. Solids Structures* **6**, 69–90.
- Mukai, D., Ballarini, R. and Miller, G. R. (1990). Analysis of branched interface cracks. *ASME J. Appl. Mech.* **57**, 887–893.
- Muskhelishvili, N. I. (1953). *Some Basic Problems in the Theory of Elasticity*. Noordhoff, Leyden, The Netherlands.
- Pak, R. Y. S. and Gobert, A. T. (1990). On the axisymmetric interaction of a rigid disc with a semi-infinite solid. *J. Appl. Math. Physics (ZAMP)* **41**, 684–700.
- Selvadurai, A. P. S. (1976). The load–deflexion characteristics of a deep rigid anchor in an elastic medium. *Geotechnique* **26**, 603–612.
- Sherman, D. I. (1940). The mixed problems of potential theory and of the theory of elasticity for the plane with a finite number of straight cuts. *Comptes Rendus de L'Academie des Sciences de L'U.R.S.S.* **27**, 330–334.